Adsorption (2024) 30:729–746
https://doi.org/10.1007/s10450-024-00465-8

Synthesis of Na-Alginate templated Montmorillonite-Silica Composite as adsorbent for removal of Rhodamine B

İlyas Deveci[1]

Received: 9 February 2024 / Revised: 24 March 2024 / Accepted: 25 March 2024 / Published online: 13 April 2024

Abstract
In this study, mesoporous Montmorillonite-Silica composites prepared by using different amount Alginate as sacrificial template, for removal of Rhodamine B is investigated. By alternating Alginate amount it is aimed to switch the porosity of adsorbents thus the adsorption capacities of adsorbents. Synthesized adsorbents had been characterized by using Scanning Electron Microscopy, X-ray diffraction, Fourier transform infrared spectroscopy and N_2-Ads/Des techniques. It is observed that beside the decrease in the micropore volume, the total pore volume of the adsorbents increased with the increasing of used Alginate amount. The total pore volumes of adsorbents synthesized with different Clay/Alginate ratio (10, 5, 1) were found as 0.116, 0.172, and 0.178 cm^3/g, respectively. Batch adsorption studies showed that the maximum removal efficiencies were obtained at acidic conditions and the adsorbents had better fit with Freundlich isotherm. Qm values obtained from Langmuir isotherm were found as 24.47, 31.97 and 28.48 mg/g for synthesized adsorbents. Also, adsorption kinetic studies showed that for all adsorbents, experimental data had good fit to the pseudo-second order kinetics model. The model parameters were found as 5.9,6.3 and 6.5 (10^{-3} g/ (mg min). Thermodynamic parameters were also investigated in the study. Negative ΔG^o values pointed out that the adsorption of RhB onto synthesized adsorbents was favorable process. Positive values of ΔHo and ΔS indicated that the adsorption of RhB on adsorbents were endothermic and rising of randomness during the adsorption of RhB on the surface of the adsorbent. Adsorbents could be recovered at least five times without significant decrease in adsorption capacity.

Keywords Alginate · Mesoporous Adsorbents · Na-montmorillonite · Error Analysis

1 Introduction

Potable water is rare and critical sources for many countries, because of the importance of it in agriculture and daily life. Especially the countries in arid climate zone, have limited potable water sources. Nearly half billion people living in 29 countries are experiencing water scarcity[1]. Water scarcity could be defined as a situation where the available water supply is much lower than the demand for water. In addition to these, water pollution caused by human activity and industry makes this problem even more inextricable. Organic and inorganic chemicals frequently used in industry such as heavy metals and organic dyes are toxic and harmful to the environment. More seriously, the fact that these chemicals are not biodegradable makes the environmental problems caused from these pollutants long-term and extensive. Moreover, wastewater containing organic dyes produced in huge volume from industries which needs coloring their products, such as textile, paper, tannery, and paint causes low light penetration and decrease in photosynthetic activity in aquatic areas[2]. Beside these, the side products could occur during the degradation of dyes in aquatic media and this may cause many complications, because of harmful and toxics nature of these products[3].

Up to date, coagulation and flocculation[4, 5], reverse osmosis[6], advanced oxidation process[7, 8], and adsorption[9] methods have been tested by using various kind of organic dyes, pesticides and antibiotics for water treatment. Adsorption could be the most cost effective and feasible method among others. In contrary to some other methods, adsorption could remove both inorganic and organic contaminant in less space and short time[10]. Adsorption

✉ İlyas Deveci
ideveci@ktun.edu.tr

[1] Department of Chemistry and Chemical Processing Technologies, Vocational School of Technical Sciences, Konya Technical University, Konya, Turkey

could be briefly defined as attachment of species that is considered as contaminants on surface of porous solid matrices. There are many types of adsorbents reported in the literature for the adsorption of organic molecules and inorganic species. Both commercial activated carbon from coal and its derivatives derived from natural sources have been used for several decades for this purpose [11]. Especially, usage of commercial activated carbon is not preferable because of its high cost and its regeneration problem. Like activated carbon, zeolites both natural and synthetic ones, have been used for adsorption of dyes and heavy metals for several decades. Mesoporous zeolites such as MCM-41, have been used as absorbent because of its high surface area and well-defined pore structure since the first discovery of it in 1992[12, 13]. Zeolites are good candidates for removal of organic pollutants from wastewater, but the use of high-cost surfactants in the production of zeolites and the fact that most of these surfactants are petroleum-based, are the main disadvantages of synthetic zeolites. Beside the adsorbent mentioned above, clays and clay-based adsorbent extensively used as adsorbent for removal of contaminants from wastewater [14–17]. Biopolymer-based adsorbents with their suitable active centers have attracted too much attention for wastewater treatment, recently. For this purpose, biopolymers, such as chitosan[18, 19], cellulose[20], dextrin[21], alginate[22] etc. and composites of them have been used extensively as adsorbent for decontamination of the wastewater. There are many studies in the literature on the adsorption applications of biopolymer clay and biopolymer pillared clay composites [23–27]. In these studies, alginate was used as a polymer matrix for the formation of beads. In our study, unlike previous studies, alginate was used as a sacrificial template as a pore change dictating agent for the first time. To our knowledge, this will be the first in the literature. In this study, findings on the synthesis of high surface area and mesoporous Montmorillonite-Silica composites in which alginate, a natural polymer, used as a sacrificial template is presented. Three different concentrations of alginate were used for differing of porosity of adsorbent. Resulting adsorbent were characterized by using attenuated total reflectance Fourier transform infrared (ATR-FTIR) spectroscopy, scanning electron microscopy (SEM), nitrogen adsorption isotherms (N_2-Ads/Des) and X-ray Diffraction (XRD). For the evaluation of interaction between dye molecules and adsorbent, the effects of different adsorption parameters such as pH, contact time and initial dye concentration, were investigated. Also, adsorption kinetic studies, error analysis, adsorption isotherms studies and determination of different thermodynamic parameters were performed for deep evaluation of adsorbent. Rhodamine B (RhB) was used as model contaminant.

2 Experimental

2.1 Materials

Hydrophilic Montmorillonite clay (Na-MMT, Sigma-Aldrich), Sodium alginate (Sigma-Aldrich) and Tetraethyl orthosilicate (TEOS, Sigma-Aldrich) were used for synthesis of adsorbent, and Rhodamine B (RhB, Sigma-Aldrich) was used as model contaminant.

2.2 Synthesis of Alginate templated MMT-Si composite adsorbent

For synthesis of adsorbents, firstly 2 g of Na-MMT was dispersed in 100 ml of water and stirred vigorously for 24 h. At the same time, certain amounts of alginate (0.2, 0.4 and 2 g) were added in 100 ml of distillated water and obtained mixture was stirred until a homogeneous solution was formed. The resulting alginate solution and Na-MMT dispersion were mixed in equal volumes. The final mixture included clay/alginate ratio was 10, 5, and 1 respectively, and was left at room temperature overnight with vigorous stirring. After then, silica sol was added into each resulting mixture. Silica sol was prepared by sol–gel technique as reported previously in literature[28]. For this purpose, TEOS, 2 N HCl and absolute ethanol were mixed in the ratio 41.6 g/10 ml/12 ml respectively and obtained sol was stirred for 2 h. SiO_2-sol added mixture was stirred vigorously for 24 h. Then obtained gel like mixture was filtered and washed with water and ethanol respectively. Obtained wet cakes were dried overnight at 80 °C then calcinated at 600 °C for 6 h.

2.3 Characterization

The prepared adsorbents were characterized by using ATR-FTIR, SEM–EDX, N_2-Ads/Des and XRD techniques. ATR-FTIR spectra of the adsorbents were recorded by using Thermo Scientific Nicolet iS20 FTIR Spectrometer within the range of 500–4000 cm^{-1}. Surface morphology of the adsorbents was investigated by using the Scanning Electron Microscope (ZEISS Gemini SEM 500). Textural properties of adsorbents such as Brunauer, Emmett and Teller (BET) surface area, total pore volume and micropore volume were obtained at 77 K by using Micromeritics/TriStar II Plus. X-Ray Diffraction spectrums of adsorbents were obtained by using X-Ray Diffractometer (Europe 600, GNR. Energy dispersive X-ray (EDX) analysis was performed by using SEM–EDX (Hitachi – SU 1510).

2.4 Adsorption studies

All experiments were performed in a temperature-controlled water bath and the initial pH of the solution was adjusted using 0.1 M NaOH or 0.1 M HCl solutions. In a typical adsorption run, 50 mg dried adsorbent was added into 25 ml of RhB solutions with different concentrations (5–75 ppm), shake for 3 h to reach the equilibrium. After 3 h, adsorbent was separated and the concentration of RhB was determined by using UV–Vis spectrophotometer at wave length of 556 nm. In this study, parameters affecting adsorption such as contact time, initial dye concentration, initial pH of solution, were investigated. Adsorption capacity of the adsorbent (Q_e) and percentage of removal of RhB (%R) were determined by using the Eqs. 1 and 2, respectively. where Q_e is the adsorption capacity of the adsorbents (mmol/g), C_0 and C_t are the initial and concentrations (mol/L) of the RhB at time t, in the solution, V (mL) is the volume of solution, and m is the amount of adsorbent used (g).

$$Qe = \frac{(C_0 - C_t) \times V}{m} \tag{1}$$

$$\%R = \frac{(C_0 - C_t)}{C_0} \times 100 \tag{2}$$

2.5 Error analysis

The error functions are valuable tools used for estimating model parameters and determining the convenience of the non-linearized models with experimental results[29, 30]. In this study, to confirm the ideal fitting of the adsorption isotherm and kinetic models with experimental results, the several error functions such as, Residual Sum of Squares Error (ERRSQ/SSE), Chi-square ($\chi 2$), Coefficient of determination (R^2), Average Relative Error (ARE), Hybrid Fractional Error Function (HYBRID), Marquardt's Percent Standard Deviation (MPSD) and Root Mean Square Error (RMSE) were used. Error functions used in this study are seen in Eqs. 3–9 and in these equations $q_{e,exp}$ is experimentally determined adsorption capacity of the adsorbents, $q_{e,cal}$ is calculated value of adsorption capacity of the adsorbents from model, n is the number of data points and p is the number of model parameters.

$$\text{ERRSQ/SSE} = \sum_{i=1}^{n} (q_{e,exp,} - q_{e,cal})^2 \tag{3}$$

$$\text{ARE} = \frac{100}{n} . \sum_{i=1}^{n} \left(\frac{(q_{e,exp,} - q_{e,cal})}{q_{e,exp,}} \right) \tag{4}$$

$$\text{HYBRID} = \frac{100}{n-p} . \sum_{i=1}^{n} \left(\frac{(q_{e,exp,} - q_{e,cal})}{q_{e,exp,}} \right) \tag{5}$$

$$\text{MPSD} = 100 \sqrt{\frac{1}{n-p} . \sum_{i=1}^{n} \left(\frac{(q_{e,exp,} - q_{e,cal})}{q_{e,exp,}} \right)^2} \tag{6}$$

$$\text{RMSE} = \sqrt{\frac{\sum_{i=1}^{n} (q_{e,exp,} - q_{e,cal})^2}{n-p}} \tag{7}$$

$$R^2 = 1 - \frac{\sum_{i=1}^{n} (q_{e,exp,} - q_{e,cal})^2}{\sum_{i=1}^{n} (q_{e,exp,} - \overline{q_{e,cal}})^2} \tag{8}$$

$$\text{Chi} - \text{square}/\chi 2 = \sum_{i=1}^{n} \frac{(q_{e,exp,} - q_{e,cal})^2}{q_{e,exp,}} \tag{9}$$

3 Results and discussions

3.1 Characterizations

SEM images of prepared alginate templated MMT-Si composite adsorbents is shown in Fig. 1. As seen in the figure, the layered structure was observed in all adsorbent structures. As it was well known that montmorillonite clay consists of overlapped layers which includes octahedral Al_2O_3 sheets sandwiched between two tetrahedral SiO_2 sheets. In general, these stacked layers are aligned randomly, and porous card-house structure is formed. But for the adsorbents synthesized in this study, the montmorillonite layers were seemed to be aligned parallel to each other due to viscous forces, during the dispersion of clays in alginate solutions. As seen in figures, the layers parallel to each other had twisted shape and the curvature of layers increased with the increasing of alginate concentration. After calcination of the adsorbent, alginate was removed from the composite, this resulted in formation of porous structure.

Elemental compositions of Na-MMT and synthesized Alginate templated MMT-Si composite adsorbents were determined by using EDX analysis and the obtained results were listed in Table 1. EDX analysis indicate that the all the samples consisted of oxides such as SiO_2, Al_2O_3, MgO and FeO. As seen in Table 1, the increase in the amount of Si in the synthesized samples compared to Na-MMT is an important result showing that Si is integrated into the structure. A correct interpretation cannot be made with elemental amounts, especially after the integration of SiO_2 into the structure. Therefore, instead of elemental amounts, it is a

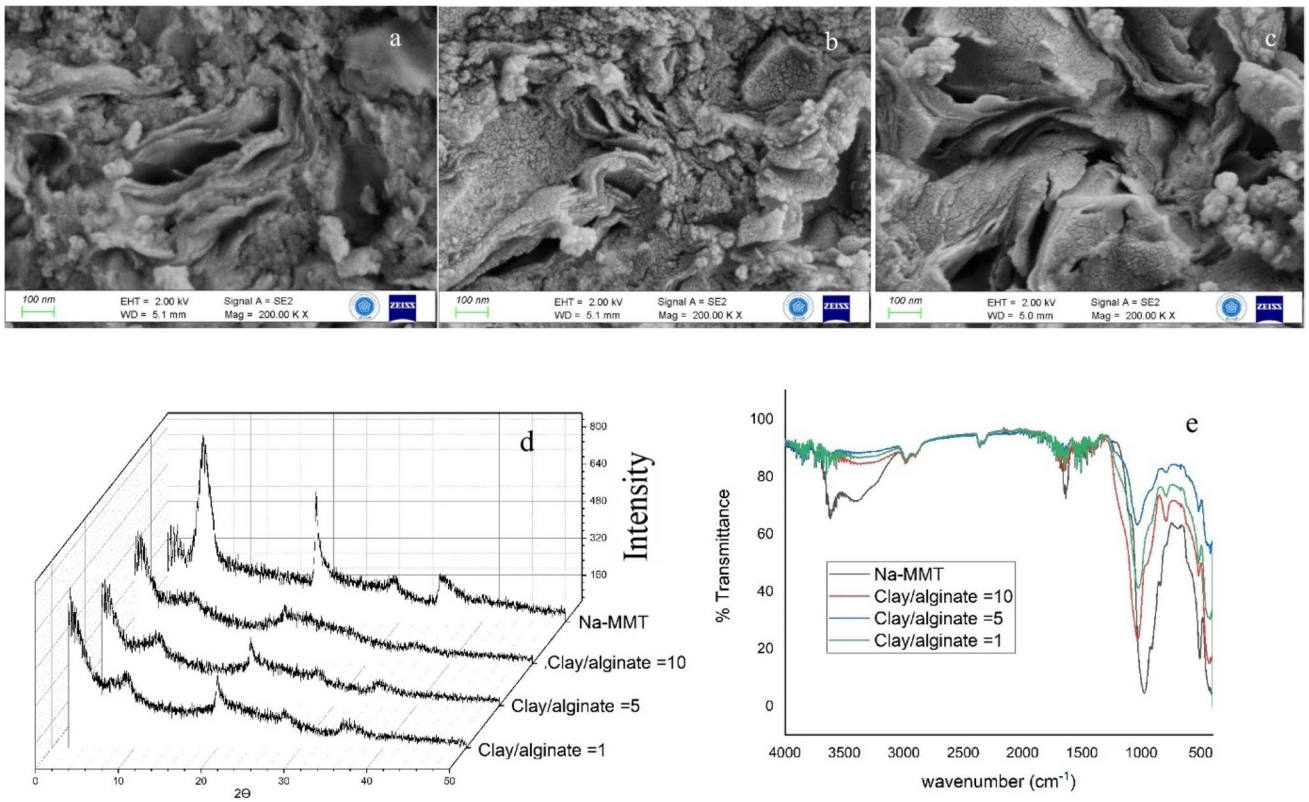

Fig. 1 SEM images of Alginate templated MMT-Si composite adsorbents (clay/alginate ratio: (**a**) 10, (**b**)5, and (**c**) 1), XRD spectrums of Alginate templated MMT-Si composite adsorbents (**d**) and FTIR spectra of Na-MMT and Alginate templated MMT-Si composite adsorbents (**e**)

Table 1 BET surface areas. Total pore volumes, Micropore Volumes and EDX results of Na-MMT and synthesized Alginate templated MMT-Si composite adsorbents

Elements	Sample (% Weight)			
	Na-MMT	Clay/alginate = 10	Clay/alginate = 5	Clay/alginate = 1
O	61.61	64.98	65.69	66.22
Mg	3.07	1.04	1.62	1.65
Al	8.46	3.20	4.98	5.07
Si	22.09	27.81	25.80	25.41
Ca	1.26	0.26	0.25	0.21
Fe	1.95	0.67	0.94	0.96
Si/Al	**2.61**	**8.69**	**5.18**	**5.01**
BET Surface Area (m^2/g)	1.9*	205.22	236.43	228.52
Total Pore Vol. (cm^3/g)	0.004*	0.116	0.172	0.178
Micropore Vol. ($cm^{3/}g$)	-	0.062	0.052	0.047

* Obtained from the literature for Na-MMT [13]

more accurate approach to interpret it based on Si/Al ratios, assuming that the amount of Al in the structure remains constant. While the Si/Al ratios found in EDX analysis of Na-MMT was found as 2.61, the same ratio obtained for Alginate templated MMT-Si composite adsorbents synthesized with different Clay/Alginate ratio (10, 5, 1) were found as 8.69, 5.18, and 5.01, respectively. Si/Al ratios decrease with the increasing of alginate used for preparation of adsorbents. This result indicates that the sites where SiO_2 structures can bond are occupied by alginate, and the number of occupied areas is directly proportional to the amount of alginate.

Figure 1(d) shows the XRD patterns of synthesized adsorbents and Na-MMT. The d_{001} value which indicate the distance between two separate layers of clay minerals,

gives valuable information about the change in basal space of Na-MMT before and after modifications. The d_{001} value could be calculated by using Bragg Eq. ($2d_{001}\sin\Theta = n\lambda$). A sharp peak at 2-theta about 6.315°, with the basal space of 1.41 nm was observed in the raw clay. On contrary, the sharp peaks correspond to 001 plane did not observe for alginate templated MMT-Si composite adsorbents. These findings showed that the clay layers were exfoliated after modifications. But also, after modification, there were broad peaks like shoulders observed for all adsorbent systems at around $2\Theta = 8.6$. These showed that not all of clay segments were exfoliated and distance between some interlayers of clays were decrease due to removal of water during the calcination.

FTIR spectra of the Na-MMT and the alginate templated MMT-Si composite adsorbent is seen in Fig. 1(e) FTIR was used for investigating the changes in chemical structures of Na-MMT before and after the modifications. As seen in Fig. 1(e), the FTIR spectrums of the Na-MMT and the modified samples were nearly identical except for the intensities of some peaks. There was no additional peak observed and it was concluded as the chemical structure of raw clay preserved after the modifications. The broad peak at around 3625 cm^{-1} could be attributed to the stretching band of –OH groups attached to the Si and Al. The peak at around the 3410 cm^{-1} is assigned to –OH stretching band for physically adsorbed water on interlayer of Na-MMT. After calcination, for all synthesized adsorbents, intensities of these peaks were decrease sharply due to removal of physically adsorbed water and degradation of –OH groups. The sharp peaks observed for all samples at 1030 cm^{-1} could be attributed to Si–O-Si stretching vibrations and the peaks at 516 cm^{-1} were assigned to Si–O bending vibrations. The absence of any peak that may belong to alginate in the FTIR spectrum indicates that the alginate is completely removed from the structure.

The textural properties of synthesized Alginate templated MMT-Si composite adsorbents are listed in Table 1. The BET surface areas of adsorbents synthesized with different Clay/Alginate ratio (10, 5, 1) were found as 205.22, 236.43 and 228.52 m^2/g, respectively. These values were much higher than the that of Na-MMT (1.9 m^2/g)[31]. On the other hand, the number of active centers on the surface and the accessibility of these centers by adsorbed materials are other important parameters. The total pore volumes of adsorbents synthesized with different Clay/Alginate ratio (10, 5, 1) were found as 0.116, 0.172, and 0.178 cm^3/g, respectively Clays are multi-layered minerals found abundantly in nature. Each layer of clay consists of an octahedral Al_2O_3 layer sandwiched between two tetrahedral SiO_2 layers. There are exchangeable cations such as Na^+, Ca^{+2} and physically adsorbed water between the layers[17]. In this study, the surface properties of clay minerals such as surface area, micro and mesopore distribution were tried to be changed by replacing the exchangeable cations between the layers with SiO_2 particles as intercalating agents. The amount of exchanged intercalating agents differs the size of the pores in resulting adsorbents. It was observed that the total pore volume of synthesized adsorbents had increased with increase in amount of the alginate used for preparation. In parallel with our expectations, it was observed that the micropore volumes of adsorbent decreased with the increasing of alginate used. These could be concluded that when the alginate which was used as sacrificial template was removed during the calcination, the remaining space formed pores. Up to a certain point, the increase in porosity help to increase the surface area but higher concentration of alginate leads to decrease in microporosity thus decrease in BET surface area. This observation was parallel to the results of EDX analysis of synthesized adsorbents. The ratio between the Si/Al ratios decreased with the decrease of Clay/Alginate ratios. This result indicates that the increase in amount of alginate reduced the amount of intercalation of SiO_2.

3.2 Adsorption studies

3.2.1 Effect of operating parameters

The effects of different adsorption parameters such as pH, contact time, and initial dye concentration, on removal of dye molecules were investigated in this study. The obtained results is shown in Fig. 2.

To investigate the effect of initial pH of solution on adsorption capacity and the percentage of removal, the solutions with different pH ranged between 2–12 were prepared. Initial pH of the solution was adjusted by using 0.1 M NaOH and 0.1 M HCl solutions. The other parameters such as contact time (120 min.), temperature (25 °C), the volume of solution (50 ml), adsorbent dosage (0.05 g) and initial dye (15 ppm) concentration were kept constant in all experiments. Figure 2(a) illustrates the effect of initial pH of the solutions on the removal efficiency. As seen in figure, the removal efficiencies of all adsorbents showed nearly same characteristics for all adsorbents in all pH values. For all adsorbents, the removal efficiencies were remained constant in pH range between 4–8. A decrease in removal efficiency was observed with increase in pH between pH ranges 2–4 in acidic conditions. Parallel to this, removal efficiencies decreased with increase in pH between pH ranges 8–12 under basic conditions. This observation showed that the interaction between the dye molecule and the surface were similar in each of the adsorbents. The highest removal efficiencies were observed at pH 2 for all adsorbents. The removal efficiencies were found as 81.05%, 95.82% and 95.41% for adsorbents synthesized with different Clay/Alginate ratio (10, 5, 1), respectively. It was reported that the

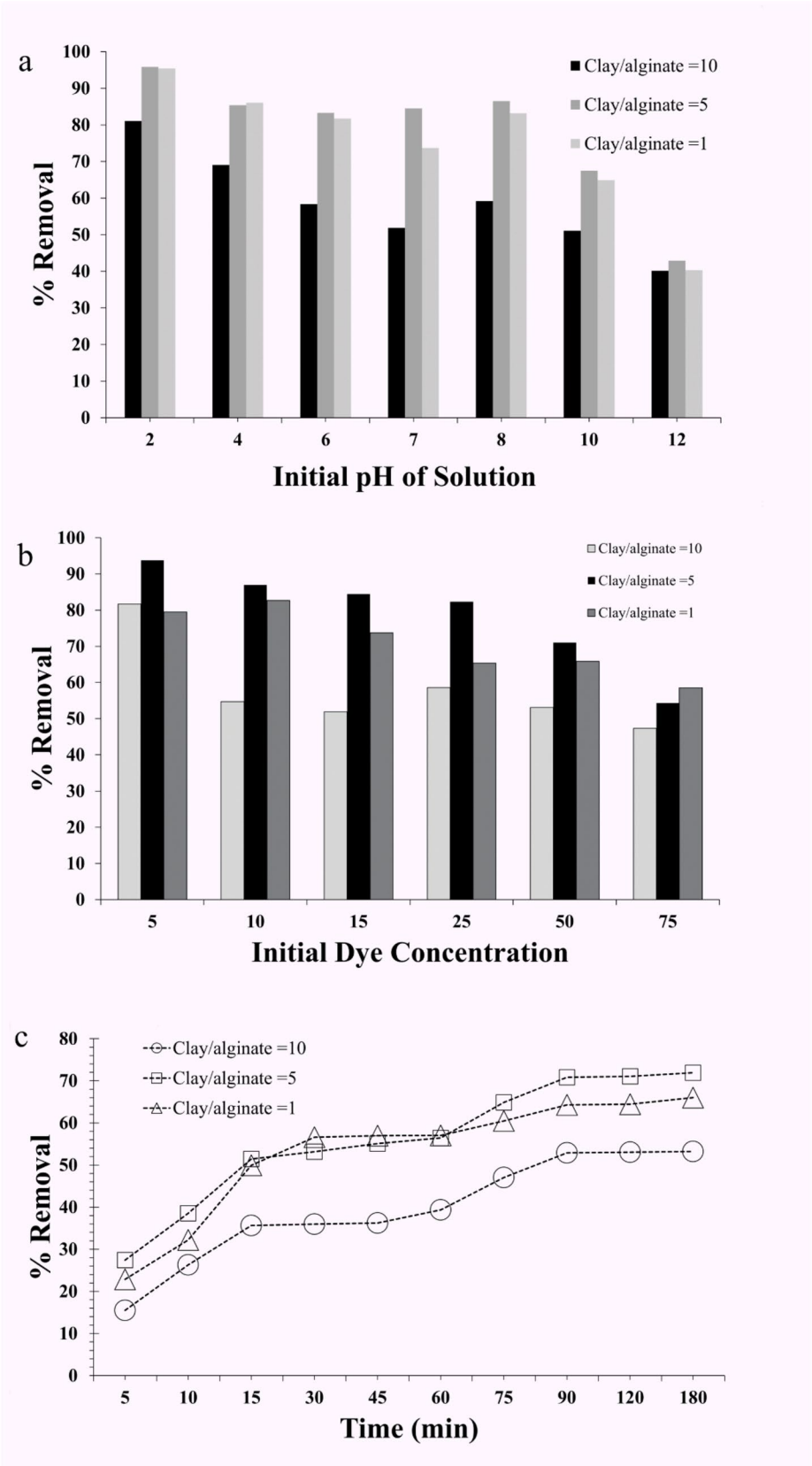

Fig. 2 The effects of operating parameters on removal efficiencies of Alginate templated MMT-Si composite adsorbents

pKa of the RhB molecules is 3.7 [32]. At lower pH values than 3.7, proton belonging to RhB acid sites do not ionize. At low pH range the hydrogen bond between Si–OH surface and the acid groups of RhB could increase the adsorption capacity thus it increased the removal efficiency. When pH values of the solution are higher than the pKa of RhB (3.7), molecule is in the zwitterionic form, and the net charge of the molecule is neutral. The zwitterionic form of the RhB in solution may led to dimerization and decrease in electrostatic interaction between surface and dye molecule thus decreasing removal efficiency. The lowest removal efficiencies were obtained at pH = 12 for all adsorbents. The removal efficiencies were found as 40.14%, 42.89 and 40.32% for adsorbents synthesized with different Clay/Alginate ratio (10, 5, 1), respectively. At high pH values, the protons belong to Si–OH and RhB acid sites easily ionized and electrostatic repulsions between the negatively charged surface and the dye molecules could lead dramatic decrease in adsorption capacity thus decrease in removal efficiencies for all adsorbent systems.

The removal efficiencies of the adsorbents for different initial dye concentrations (5–75 ppm) and for different contact time (0–180 min) are illustrating in Fig. 2b and Fig. 2c, respectively. For investigating effect of initial dye concentrations on removal efficiencies, experiments performed with different RhB concentrations in the range between 5–75 ppm. For this purpose, the other parameters such as contact time (120 min.), temperature (25 °C), the volume of solution (50 ml), adsorbent dosage (0.05 g) and pH (7) were kept constant. As seen in Fig. 2b decrease in the removal efficiencies is observed with the increase in initial dye concentration for all adsorbents. At low initial dye concentration, the surface coverage is low and therefore the equilibrium between adsorbed dye molecules and dye molecules in bulk solution is established at low concentration. For this reason, the ratio between adsorbed dye molecules and dyes in solution form is high at low concentrations and therefore the removal efficiency is high. The other important point observed from experimental results was that the rate of decrease in removal efficiency was higher for adsorbents synthesized with Al/clay ratio = 10 then other adsorbents. In experiments which the initial concentration was 5 ppm, the removal percentages were found to be 81.68%, 93.8% and 79.48%, respectively, for the adsorbents synthesized using the Clay/ Alginate ratios (10, 5, 1), whereas, in the experiments which the initial concentration was 75 ppm, the removal efficiencies for the adsorbents were found as 47.31, 54.34 and 58.49, respectively.

The variation of RhB removal efficiency with contact time was investigated at an initial dye concentration of 50 ppm, a sorbent mass of 0.05 g, a solution volume of 50 mL, a solution pH of 7, and a temperature of 25 °C. Figure 2c shows the removal efficiency of RhB with respect to time. As seen in the figure, the removal efficiencies of RhB for all adsorbents increased over time up to a point. It was observed that the rate of adsorption of RhB on adsorbent was fast at the early stages, but Removal efficiencies for all adsorbents was found to be reach a constant value at contact times of 90 min or little more. At this point, the amount of adsorbed and desorbed dye molecules from surface of the adsorbent is equal and the system is in equilibrium state. The removal efficiencies at equilibrium states were found as 53.2%,71.92% and 65.98% for adsorbents synthesized using the Clay/ Alginate ratios (10, 5, 1), respectively. At these specific conditions mentioned above and at equilibrium, the concentrations in bulk solution are referred as equilibrium concentrations (C_e) and the adsorbed amount of on unit mass of absorbate is referred as equilibrium absorption capacity (Q_e).

3.2.2 Adsorption isotherms

Adsorption isotherms provide important information's on adsorbate-adsorbent interaction, surface properties of adsorbent, adsorption mechanism, and have been frequently studied in the literature. In this study, equilibrium adsorption data were analyzed using three adsorption isotherms such as Langmuir, Freundlich and Sips. The experimental equilibrium adsorption data and the fitted curves obtained by using the nonlinear form of Langmuir, Freundlich and Sips isotherms is seen in Fig. 3. The isotherm parameters obtained by using nonlinear curves and the error values measured for each fitted curve is listed in Table 2.

The shape of the isotherms gives valuable information about the adsorption mechanism. For the obtained fitting curve of RhB adsorption onto adsorbents, the shape of the curves showed the Type L, which could be attributed to the absence of competition between the RhB and the water molecules for getting hold of absorptive sites[33].

The isotherm equations used in this study are listed in Table 2. In these equations, Q_e (mg/g) and C_e (mg/L) are adsorbed amount of dye molecules on unit mass of adsorbent and concentration of dye molecules at equilibrium state. For Langmuir isotherm model, it is assumed that the adsorbed species occupied active sites on the homogeneous surface, there is no interaction between the adsorbed molecules, also the coverage of the surface is in the form of monolayer. In Langmuir isotherm equations, K_L (L/mg) is Langmuir isotherm constant and Q_m (mg/g) is maximum adsorption capacity[34]. Freundlich isotherm is an empirical equation used for delineation of heterogeneous adsorption systems with assuming there are interactions between adsorbed molecule and on contrary to Langmuir isotherm, it is not restricted to the formation of the monolayer. In this model, K_F ($L^{1/n}\,mg^{1-1/n}g^{-1}$) is Freundlich Isotherm constant, n is the value that indicate adsorption intensity The Sips isotherm is an integrated form of Langmuir and Freundlich

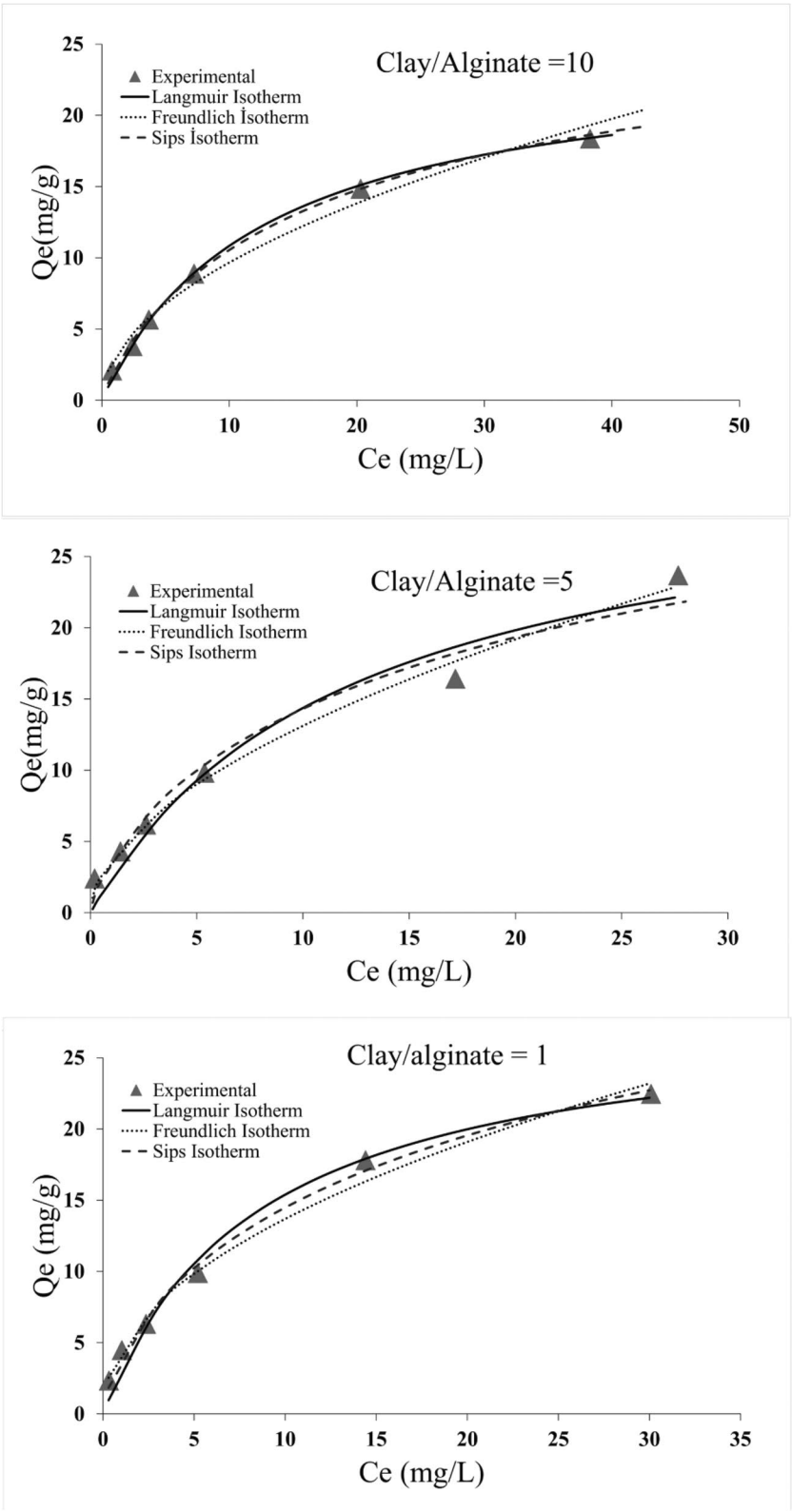

Fig. 3 Nonlinear fitting curves of Langmuir, Freundlich and Sips isotherm models and experimental equilibrium data for adsorption of RhB onto Alginate templated MMT-Si composite adsorbents (initial concentrations of RhB of 5,10,15,25,50, and 75 mg/L, adsorbent dose of 0.05 g, a solution volume of 0.05L, T = 308 K, and initial solution pH = 7)

models so sometimes it is called as Langmuir–Freundlich equation. The Sips isotherm is putted forward for identifying the adsorption in heterogeneous systems to overcome the dilemma of the continuing rising in adsorption capacity with increase of the adsorbate concentration associated with the Freundlich isotherm [34, 35]. In Sips Isotherm equation,

Table 2 Isotherm equations and Isotherm parameters of Langmuir, Freundlich and Sips models and measured error values for adsorption of RhB onto Alginate templated MMT-Si composite adsorbents

Isotherm model	Equation	Parameters	Clay/Alginate		
			10	5	1
Langmuir	$Qe = \frac{Q_m K_L Ce}{1+K_L x C_e}$	K_L	0.079	0.082	0.12
		Q_m (mg/g)	24.473	31.974	28.48
		ERRSQ(SSE)	0.50	12.29	4.46
		Chi-square/ $\chi 2$	0.01	0.69	0.52
		R2	0.99757	0.96292	0.98594
		ARE	-0.59	4.34	3.99
		RMSE	0.35	1.75	1.06
		HYBRID	-0.88	6.50	5.98
		MPSD	1.76	13.01	11.96
		SNE	**1.22**	**3.04**	**2.42**
Freundlich	$Q_e = K_F C_e^{\frac{1}{n}}$	K_F	2.95	3.713	4.54
		1/n	0.52	0.548	0.48
		ERRSQ(SSE)	3.21	3.19	3.20
		Chi-square/ $\chi 2$	0.34	0.15	0.20
		R2	0.9845	0.9904	0.9899
		ARE	-2.47	-0.87	-1.33
		RMSE	0.90	0.89	0.90
		HYBRID	-3.71	-1.31	-1.99
		MPSD	7.42	2.62	3.99
		SNE	**0.90**	**1.77**	**1.49**
Sips	$Qe = \frac{Q_m K_s (C_e)^{n_s}}{1+K_s (C_e)^{n_s}}$	Q_m	28.61	39.722	46.00
		K_s	0.08	0.100	0.10
		n_s	0.87	0.751	0.68
		ERRSQ(SSE)	0.32	9.25	1.36
		Chi-square/ $\chi 2$	0.09	1.13	0.18
		R2	0.99848	0.97211	0.9957
		ARE	1.19	4.93	2.58
		RMSE	0.32	1.76	0.67
		HYBRID	2.39	9.85	5.17
		MPSD	4.14	17.06	8.95
		SNE	**2.28**	**2.63**	**2.22**

K_s (L^{ns}/mg^{ns}) is Sips isotherm constant, Q_m (mg/g) is maximum adsorption capacity and n_s is a numerical value that represent the measure of heterogeneity of the adsorption process and limited from 0 to 1[34].

The isotherm constants and calculated error values of used isotherm models in our study were determined by a nonlinear regression method based on minimizing ERRSQ/SSE functions for each adsorbent. After then the value of error functions mentioned in Sect. 2.5 were calculated by using experimental data points and fitted isotherm models. To evaluate the fitting of used isotherm models to experimental data, it was aimed to minimize the error functions 3–9 [29]. But it was not always easy to minimize the value of each error functions for each isotherm, thus the other indicator value such as sum of normalized errors (SNE) was determined for each adsorbent. SNE values was calculated by using the procedure reported in literature [36]. The minimum SNE value indicates the lowest value of summation of the scaled errors thus it specifies the best fitting of isotherm models to experimental data. As seen in Table 2 lowest SNE values for each adsorbent was obtained for Freundlich isotherm model. As seen in Table 2, K_f values of Freundlich isotherm gradually increased with the increasing of Clay/Alginate ratio used for preparing adsorbents. Also $1/n_f$ values were determined as 0.52 0.548 and 0.48 for adsorbents synthesized using the Clay/Alginate ratios (10, 5, 1), respectively. Due to the random distribution of different functional groups in natural materials, chemical homogeneity cannot be expected on their surfaces [37]. Clay, a natural material, is known to be chemically heterogeneous [38]. The surface properties of adsorbents vary with the amount and distribution of atoms on the surface. The adsorbents obtained in this

study generally contain -Si–O and Si–OH groups on their surfaces. It is known that Si–OH groups increase the hydrophilic character on the surface of the adsorbent, while Si–O groups increase the hydrophobic feature on the surface of the adsorbent[39]. In addition, with heat treatment, Si–OH groups on the surface can lose water and form Si–O-Si structures. In addition to the amount of groups with hydrophobic and hydrophilic characters, how these groups are distributed on the surface determines the properties of the surface. In this context, the raw material used, and the method applied in the development of adsorbent systems may have caused a heterogeneous surface to be obtained. Therefore, it is not surprising that the Freundlich isotherm, which accepts heterogeneous active center distribution, is the most suitable isotherm for RhB adsorption on the developed adsorbents. For the developed adsorbent systems, the $1/n_f$ value is less than 1, indicating that the surface is saturated with adsorbent and the adsorption of RhB on synthesized adsorbent was found as favorable.

Besides that, although the Langmuir isotherm model is not the best-fit isotherm, it still provides important information about the adsorbent such as Q_m which could be denoted as maximum adsorption capacity. Qm values was found as 24.47, 31.97 and 28.48 mg/g for adsorbents synthesized using the Clay/Alginate ratios (10, 5, 1), respectively. Q_m values were observed to be proportional with the BET surface areas of related adsorbents. Qm values could also be calculated by using Sips isotherm. As seen in Table 2, Q_m values were proportional to the increase in Clay/Alginate ratio used for preparing adsorbents. Q_m values was found as 28.61,39.722 and 46.00 mg/g for adsorbents synthesized using the Clay/Alginate ratios (10, 5, 1), respectively. Q_m values computed by using Sips isotherm for all adsorbents were higher than the Q_m values of adsorbents calculated by using the Langmuir isotherm.

3.2.3 Adsorption kinetics

Adsorption kinetics, which provides essential information about the efficiency of the process and the adsorption mechanism, has a remarkable importance in adsorption studies. The applicability of adsorbents in industrial processes of and the comparison of adsorbents with other adsorbents reported in the literature require a good knowledge of the kinetic parameters of the developed adsorbent systems. There are several kinetic models used for investigating adsorption rate [40, 41]. In this study kinetic models such as Pseudo First Order Kinetic Model (PFO), Pseudo Second Order (PSO) Kinetic Model, Intra-Particle Diffusion (IPD) Model and Elovich model were employed for investigating adsorption kinetic of RhB onto the Alginate templated MMT-Si composite adsorbents. Nonlinear form of the kinetic model equations was used for examining adsorption kinetics. The experimental adsorption data with respect to time and the fitted curves obtained by using the nonlinear form of kinetic models is seen in Fig. 4 for all adsorbents. Fitting parameters of proposed model, error values calculated by using error functions mentioned previous sections and investigated model equations are listed in Table 3. For the PFO and PSO equations presented in Table 3, q_e and q_t are the amount of RhB sorbed on unit mass of synthesized adsorbents, at equilibrium state and time t. k_1 (min^{-1}) and k_2 (g mg^{-1} min^{-1}) represents the rate constants of PFO and PSO kinetic models, respectively. For the IPD model, k_{id} is defined as IPD rate constant (mg g^{-1} $min^{-1/2}$) and C is a constant associated with the measure of the influence of boundary layer. For the Elowich kinetic model equations, α is defined as initial rate of adsorption ($mg{\cdot}g^{-1}{\cdot}min^{-1}$) and β ($g{\cdot}mg^{-1}$) is a constant corelated with the activation energy of the reaction took place between adsorbate and adsorbent, and the degree of surface coverage of dye molecules.

To validate the viability of kinetic models used in this study in fitting to experimental data, SNE values was calculated by using same methodology applied in isotherm studies. In this manner, it was aimed to achieved lowest error values which indicate the best fit. As seen in Table 3, lowest SNE values were obtained for PSO kinetic model for all adsorbents. PSO model is assuming that the rate-limiting step comprise chemical adsorption known as strong interactions between dye molecules with adsorbate [42]. As seen in Fig. 4, for all adsorbents, instantaneous sorption of RhB within the first 15 min of adsorption process was observed, and this could be attributed to high affinity between RhB molecules and the adsorbent surface. After 15 min, the rates of adsorption decreased due to increase in surface coverage and adsorption process reached equilibrium at just about 90 min, for all adsorbents. Experimentally observed qe values were found to be very close to qe values obtained from the PSO model. Experimentally observed qe values were found to be 13.26, 17.75 and 16.11 mg/g for adsorbents synthesized using the Clay/Alginate ratios (10, 5, 1), respectively. By the way, qe values obtained from the PSO model were computed as 13.71 18.15 and 17.29 mg/g for adsorbents with same order. Obtained results were in good agreement with the textural properties of the adsorbents. It was seen that the qe values were proportional with the surface areas of the adsorbents. The PSO rate constant (k_2) were also calculated from model fit equations. k_2 values were found as 0.0059, 0.0063 and 0.0065 for adsorbents synthesized using the Clay/Alginate ratios (10, 5, 1), respectively. The other important values that could obtained from the PSO model is the initial adsorption rates (h, mg g^{-1} min^{-1}). Initial adsorption rate is represented by Eq. 10 where k_2 is PSO rate constant and $q_{e,\,cal}$ is calculated equilibrium quantity from PSO model of RhB adsorbed on unit gram of adsorbent.

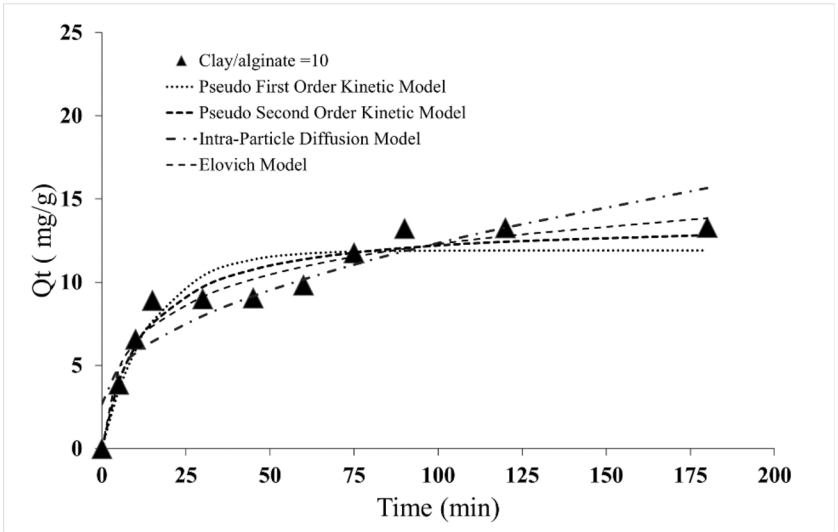

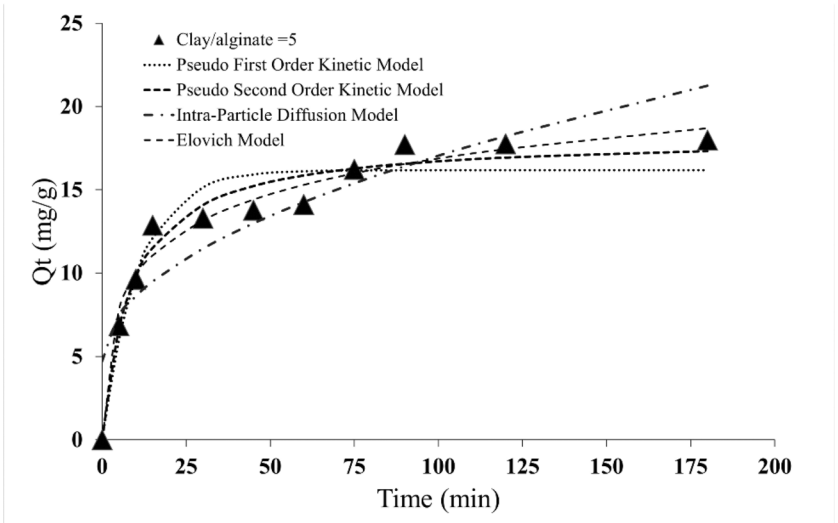

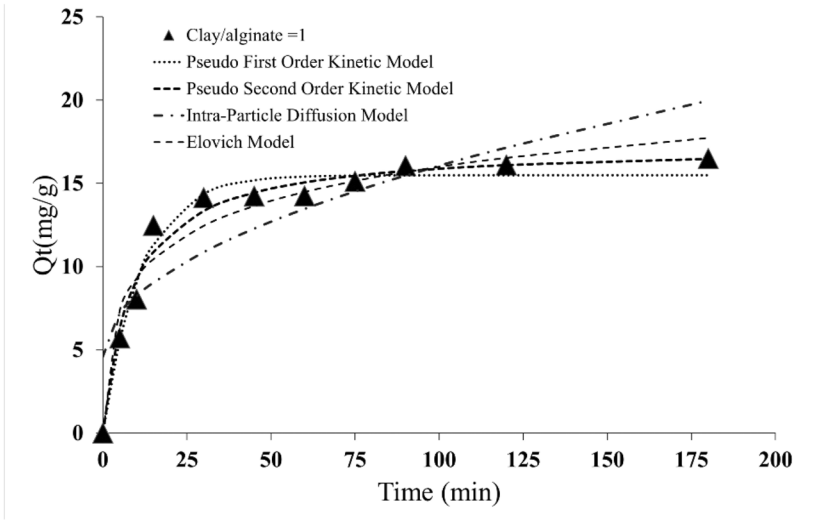

Fig. 4 Nonlinear fitting curves of Kinetic models and experimental data for adsorption of RhB onto Alginate templated MMT-Si composite adsorbents (initial concentrations of RhB of 50 mg/L, adsorbent dose of 0.05 g, a solution volume of 0.05L, T = 298 K, and initial solution pH = 7)

Table 3 Kinetic model equations. Kinetic model parameters and measured error values for adsorption of RhB onto Alginate templated MMT-Si composite adsorbents

Kinetic model	Equation	Parameters	Clay/Alginate		
			10	5	1
Pseudo First Order Kinetic Model	$q_t = q_e(1 - e^{k_1 t})$	k_1 (min^{-1})	0.068	0.092	0.087
		qe (mg/g)	11.912	16.181	15.491
		ERRSQ(SSE)	18.57	21.57	6.51
		Chi-square/2	1.88	1.50	0.51
		R2	0.8945	0.92791	0.97653
		ARE	0.90	0.48	-0.45
		RMSE	2.15	2.32	1.28
		HYBRID	1.35	0.72	-0.68
		MPSD	3.11	1.66	1.56
		SNE	**1.51**	**1.31**	**1.34**
Pseudo Second Order Kinetic Model	$q_t = \frac{k_2 q_e^2 t}{1+k_2 q_e t}$	k_2 (g/(mg min)	0.0059	0.0063	0.0065
		qe (mg/g)	13.715	18.152	17.292
		ERRSQ(SSE)	10.18	10.13	5.68
		Chi-square/2	1.04	0.71	0.52
		R2	0.9422	0.96613	0.9795
		ARE	-0.66	-0.13	-1.89
		RMSE	1.60	1.59	1.19
		HYBRID	-0.99	-0.19	-2.84
		MPSD	2.28	0.44	2.81
		SNE	**1.32**	**1.24**	**1.14**
Intra-Particle Diffusion Model	$q_t = k_{id} t^{\frac{1}{2}} + C$	k_{id}	0.967	1.233	1.146
		C	2.674	4.704	4.588
		ERRSQ(SSE)	24.07	52.29	64.08
		Chi-square/2	1.77	2.10	3.23
		R2	0.863	0.825	0.769
		ARE	3.55	6.41	3.89
		RMSE	2.45	3.62	4.00
		HYBRID	5.33	9.62	5.83
		MPSD	12.30	22.21	13.46
		SNE	**2.06**	**1.84**	**1.47**
Elovich model	$q_t = \frac{1}{\beta}\ln(\alpha\beta t + 1)$	α	2.61	7.02	6.48
		β	0.37	0.32	0.34
		ERRSQ(SSE)	7.79	8.05	13.47
		Chi-square/2	0.89	0.63	1.34
		R2	0.9558	0.9731	0.9514
		ARE	-2.65	-1.35	-3.54
		RMSE	1.40	1.42	1.84
		HYBRID	-3.98	-2.02	-5.31
		MPSD	9.18	4.65	12.25
		SNE	**1.38**	**1.41**	**1.49**

$$h = k_2 \times q_{e,cal}^2 \tag{10}$$

The initial adsorption rates were found as 1.11, 2.09 and 1.95 mg g^{-1} min^{-1} for adsorbents synthesized using the Clay/Alginate ratios (10, 5, 1), respectively. It was observed that, the initial adsorption rates of adsorbents were proportional with the surface area of the adsorbents. The obtained results indicates that the main driving force of RhB adsorption on synthesized adsorbents was surface area of the adsorbents.

3.2.4 Effect of temperature and adsorption thermodynamics

The other important parameter which had great impact on adsorption process is temperature. To investigate the effect of temperature on the removal efficiency, experiments at 3 different temperatures (298 K, 308 K and 318 K) were carried out while keeping other parameters such as initial concentration of solution (75 ppm), initial solution pH (7), solution volume (50 ml) and adsorbent amount (0.05 g) constant. The removal efficiencies of adsorbents with respect to temperature is seen in Table 4. As seen in table removal efficiencies for all adsorbents increase with increasing of temperature. This may be mainly due to the increase in mobility of the dye molecules, the decrease in the solution viscosity, and therefore the decrease in the diffusion restrictions at boundary layer and in the pores of adsorbent.

Gibbs free energy (ΔG^o), standart enthalpy (ΔH^o) and standard entropy (ΔS^o) of adsorption of RhB on adsorbents were listed in Table 4. Thermodynamic parameters were computed by using equations given below:

$$K_{eq} = M_{w(T)} \frac{q_e}{C_e} \tag{11}$$

$$\Delta G^o = -RTln\left(K_{eq}\right) \tag{12}$$

$$\ln\left(K_{eq}\right) = \frac{-\Delta H^o}{RT} + \frac{\Delta S^o}{R} \tag{13}$$

where K_{eq} is the distribution coefficient, q_e is adsorbed amount of RhB on unit mass of the adsorbent (mg/g), C_e is the equilibrium concentration of RhB in solution(mg/L), $M_{w(T)}$ is the mass of water per liter at temperature T, R is universal gas constant (8.31441 J/mol·K). ΔH^o and ΔS^o of adsorption of RhB were calculated by van't Hoff plot (ln K_{eq} vs 1/T). The intercept and the slope of the plot indicates the $\Delta S^o/R$ and $\Delta H^o/R$, respectively. ΔG^o values were calculated by using Eq. 12. The Keq value must be dimensionless, so when calculating the K_{eq} value, it was assumed that RhB is dissolved in 1000 g of water and the density of the water did not change within the specified temperature range [43]. For all adsorbents, it was observed that the ΔG^o had negative sign which could be attributed to spontaneous nature of RhB adsorption on synthesized adsorbents. Also, negative ΔG^o values pointed out that the adsorption of RhB onto synthesized adsorbents was favorable process in investigated temperature range. Besides that, ΔH^o and ΔS^o of adsorption of RhB on each adsorbents had positive sign. Positive ΔH^o results indicated that the adsorption of RhB on adsorbents were endothermic and positive values of ΔS° in investigated temperature range, was connected to the rising of randomness during the adsorption of RhB on the surface of the adsorbent.

There are many studies on RhB adsorption on several adsorbents systems in literture Table 5 shows the Q_m values corresponds to RhB adsorption on several adsorbents systems. Q_m values were obtained by using Langmuir isotherm model. It was seen that, in the studies that used the Alginate beads alone, low adsorption capacities were observed for RhB removal [44–46] Although, there were the studies that used unmodified clays with high adsorption capacities as adsorbent for removal of RhB [49, 50], the swelling properties of clays could cause separation problem that made the usage of unmodified clays problematic. Also, there are several studies that used Clay-Alginate composite beads as adsorbent in literature. Montmorillonite-Alginate beads were investigated as adsorbent for removal of paraquat herbicides [51]. In this study, M. Etcheverry and coworkers concluded that the Q_m values obtained for adsorption of paraquat herbicides onto Montmorillonite—Alginate beads were inversely proportional with the increasing of Alginate amount. There are only a few studies focused on alginate templated porous inorganic materials, in literature. R. Sabarish, and G. Unnikrishnan used alginate as sacrificial template for synthesis of hierarchical

Table 4 Thermodynamic parameters of adsorption of RhB onto synthesized adsorbents at different temperatures

Adsorbent (Clay/alginate)	T (K)	Removal efficiency (%)	ΔG^o (kj/mol)	ΔH^o (kj/mol)	ΔS^o (j / molK)	R^2
10	298	47.3	-15.13	3.43	61.50	0.9266
	308	49.0	-15.81			
	318	49.5	-16.38			
5	298	54.31	-15.83	32.87	163.2	0.9914
	308	63.12	-17.29			
	318	73.28	-19.10			
1	298	58.50	-16.25	10.41	89.21	0.8925
	308	59.89	-16.94			
	318	64.77	-18.04			

Table 5 Comparison Q_m of the synthesized Adsorbents with other adsorbents used for adsorption of RhB

Adsorbent	Q_m* (mg/g)	Ref
Alginate Beads	0.6	[44]
Alginate-graphene beads	15.0	[44]
Crosslinked Alginate Beads	0.08	[45]
Alginate/Reduced Graphene Oxide Composite Hydrogels	18.4	[46]
Ordered mesoporous carbon (MOMC-x) monoliths	56.4	[47]
Commercial activated carbon	58	[48]
Sodium montmorillonite	38.27	[49]
Brazilian natural bentonite	77.3	[50]
Alginate Templated Montmorillonite-Silica Composite	31.9	**This work**

*Q_m values were obtained by using Langmuir Isotherm Model

silicalites [52]. In conclusions, the results obtained in this study, in which alginate was used as a sacrificial template, were found as comparable to the results obtained for other adsorbents developed for the removal of RhB in the literature. Although the adsorption capacity of the developed adsorbents is not as high as activated carbon and its derivatives, it could be preferred considering the thermal stability and reusability of the adsorbents. Moreover, the developed adsorbent systems have superior properties such as easy separation from solution and high surface area compared to raw clay and alginate.

3.2.5 Regeneration and reusability of the adsorbents

Other important parameters showing the effectiveness of adsorbent systems are reusability and regeneration. For both economic and environmental concerns, adsorbents are required to be long-lasting and reusable. For this purpose, dye desorption and reusability tests were carried out for the developed adsorbent systems. In desorption experiments, firstly, dye adsorption was carried out with the developed adsorbents at an initial concentration of 50 ppm at 25 °C and an initial pH of 7 for 3 h. Then, the adsorbents were

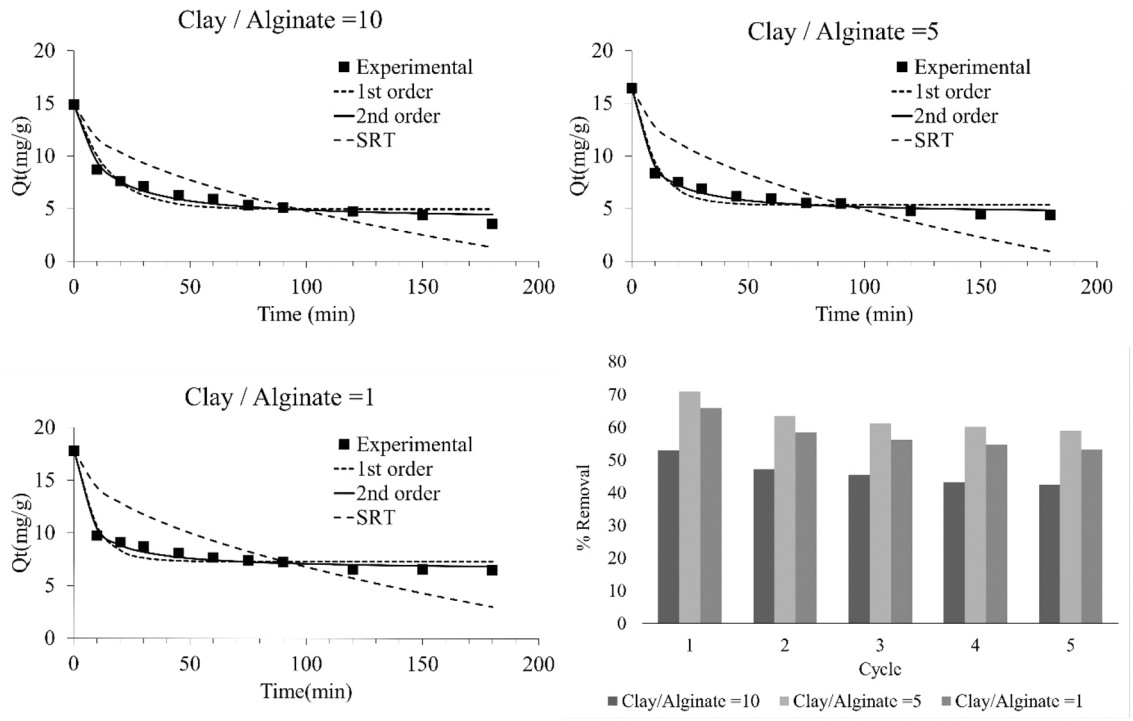

Fig. 5 Nonlinear fitting curves of Desorption Kinetic models and experimental data for desorption of RhB. Reusability chart of adsorbents

separated from the solution with the help of a centrifuge, and pure water is placed on the adsorbents and the desorption of the dye is monitored with a UV–vis spectrometer at certain time intervals. Obtained results and nom linear fitting curves are seen in Fig. 5. Desorption kinetic models such as Pseudo First Order desorption Kinetic Model (PFOD), Pseudo Second Order (PSOD) Desorption Kinetic Model [53] and Statistical Rate Theory [54], were used for investigating desorption kinetics of RhB onto the Alginate templated MMT-Si composite adsorbents. As in the adsorption kinetic studies, error analysis was performed for the desorption kinetic analysis of adsorbents. Error analysis results and used desorption model equations are listed in Table 6. For the PFOD and PSOD equations presented in Table 6, q_{eD} (mg g^{-1}) is the amount of desorbed RhB at desorption equilibrium and q_t are the amount of RhB remained on unit mass of adsorbents. k_{1D} (min^{-1}) and k_{2D} (g mg^{-1} min^{-1}) represents the rate constants of PFOD and PSOD kinetic models, respectively. Beside the classical Lagergren kinetic models Statistical Rate Theory was employed for investigating desorption kinetics. In this equation K′ is a constant. For all desorption models, q_o represents the initially adsorbed RhB, on unit mass of adsorbent systems. As seen in Table 6, lowest SNE values and highest R^2 values were obtained for PSOD kinetic model for all adsorbents. Additionally, Fig. 5 shows that the experimental results and the fitted PSOD curves are compatible. Also, it was observed that the desorption rate is initially rapid and the most of the RhB was desorbed in 10 min. The desorption process reached nearly the equilibrium state in 50 min. From fitted PSOD curve, k_{2D} values were found as 0.0087, 0.0136 and 0.0172 g/(mg min) for adsorbents synthesized using the Clay/Alginate ratios (10, 5, 1), respectively. By using Eq. 10, the initial desorption rates were found as 1.063, 1.95 and 2,18 mg g^{-1} min^{-1}

Table 6 Desorption Kinetic model equations, Desorption Kinetic model parameters and measured error values for desorption of RhB

Kinetic model	Equation	Parameters	Clay/Alginate		
			10	5	1
Pseudo First Order Desorption Kinetic Model	$q_t = q_o - q_{eD}(1 - e^{k_{1D}t})$	k_{1D} (min^{-1})	0.067	0.101	0.115
		Qe_D (mg/g)	9.90	11.06	10.49
		ERRSQ(SSE)	6.12	5.51	4.86
		Chi-square/2	1.15	0.95	0.62
		R2	0.9361	0.95219	0.95283
		ARE	-3.87	-2.82	-1.40
		RMSE	1.24	1.17	1.10
		HYBRID	-5.80	-4.22	-2.10
		MPSD	12.41	16.13	12.67
		SNE	**0.91**	**1.35**	**1.27**
Pseudo Second Order Desorption Kinetic Model	$q_t = q_o - \frac{k_{2D}q_{eD}^2 t}{1+k_{2D}q_{eD}t}$	k_{2D} g/(mg min)	0.0087	0.0136	0.0172
		Qe_D (mg/g)	11.02	11.95	11.26
		ERRSQ(SSE)	1.91	1.48	1.39
		Chi-square/2	0.37	0.25	0.17
		R2	0.9801	0.98713	0.98652
		ARE	-1.63	-0.97	-0.46
		RMSE	0.69	0.61	0.59
		HYBRID	-2.44	-1.46	-0.69
		MPSD	6.12	6.40	5.24
		SNE	**0.82**	**0.99**	**1.19**
STR Model	$q_t = q_o - q_m \times K\prime t^{\frac{1}{2}}$	qm	20.497	21.930	18.177
		K'	0.049	0.053	0.061
		ERRSQ(SSE)	35.76	52.29	70.93
		Chi-square/2	5.94	2.10	8.61
		R2	0.627	0.825	0.311
		ARE	-7.04	6.41	-13.99
		RMSE	2.99	3.62	4.21
		HYBRID	-10.56	9.62	-20.99
		MPSD	74.37	35.82	86.20
		SNE	**1.36**	**3.07**	**1.57**

for adsorbents synthesized using the Clay/Alginate ratios (10, 5, 1), respectively. At the end of 180 min, some of the RhB is still attached on the adsorbent surface. After desorption, 23.97%, 26.72% and 36.57% of the initial RhB remained on the surface, for adsorbents synthesized using the Clay/Alginate ratios (10, 5, 1), respectively.

There are basically two main methods recommended in the literature for the regeneration of adsorbents. The first method for regeneration is the recovery of adsorbed dye or heavy metal in a suitable solvent. The main concern in this method is the emergence of secondary pollutants or the high amount of solvent to be used to recover the adsorbent [55]. Another method, especially for dye adsorption, is to recover the adsorbent by applying heat treatment. In this study, heat treatment was preferred for the recovery of adsorbents. After the adsorption process, the adsorbents were separated from the solution by centrifugation, dried and heat treated at 400 oC for 3 h. The adsorption process was repeated for the recovered adsorbents, keeping the ratio between the adsorbent and the used solution volume constant. When the system reached equilibrium after 3 h, the amount of RhB was measured with a UV–Vis spectrometer and percentage removal values were determined. The results obtained are seen in Fig. 5. According to the results obtained, no significant decrease was observed in the removal percentages of the adsorbent samples after 5 successful recovery periods.

4 Conclusions

In this study, the effect of using different amounts of alginate as sacrificial template on the synthesis and porosity of mesoporous inorganic Montmorillonite-Silica composites was investigated. For this purpose, three different adsorbents were synthesized with different clay/alginate ratios (10, 5, and 1). Obtained mesoporous composites were used as adsorbent for removal RhB. N_2-Ads/Des results showed that the total pore volume of resulting adsorbents increased with the increasing of used Alginate amount. It was observed that the adsorption of RhB on all synthesized adsorbents were favorable at acidic conditions. Additionally, the batch adsorption and adsorption kinetic studies indicated that the adsorption of RhB on synthesized adsorbents had good fit to Freundlich isotherm and pseudo second order kinetic models. The non-linear form of adsorption and kinetic models had been employed to investigate the adsorption of RhB on synthesized adsorbents and six different error functions had been computed to testify the validity of the models. By using these error functions SNE values were calculated and used for describing non-linear curve fitting of proposed models. Batch adsorption studies showed that the Qm values were proportional with BET surface area of synthesized adsorbents. Qm values was found as 24.47, 31.97 and 28.48 mg/g for adsorbents synthesized using the Clay/Alginate ratios (10, 5, 1), respectively. Thermodynamic investigations indicated that the adsorption of RhB on all synthesized adsorbents were spontaneous, endothermic and the randomness were increase. Regeneration studies showed that adsorbents had significant adsorption capacity after 5 successful recovery periods It could be concluded that the using natural polymers as sacrificial template could be the good alternative for synthesizing mesoporous inorganic materials.

Author's contribution **İlyas Deveci;** Conceptualization; Data curation; Formal analysis; Methodology; Resources; Software; Validation; Visualization; Writing original draft; and Writing—review & editing.

Funding Open access funding provided by the Scientific and Technological Research Council of Türkiye (TÜBİTAK). The authors did not receive support from any organization for the submitted work. No funding was received to assist with the preparation of this manuscript.

Data availability The author confirms that the findings of this study will be made available on request.

Declarations

Ethics approval Not applicable.

Consent to participate and consent to publish Not applicable.

Competing interest The authors declare no competing interests.

References

1. Tamer, T.M., Abou-Taleb, W.M., Roston, G.D., Mohyeldin, M.S., Omer, A.M., Khalifa, R.E., Hafez, A.M.: Formation of zinc oxide nanoparticles using alginate as a template for purification of wastewater. Environ. Nanotechnology. Monit. Manag. **10**, 112–121 (2018). https://doi.org/10.1016/j.enmm.2018.04.006
2. Anastopoulos, I., Hosseini-Bandegharaei, A., Fu, J., Mitropoulos, A.C., Kyzas, G.Z.: Use of nanoparticles for dye adsorption: Review. J. Dispers. Sci. Technol. **39**, 836–847 (2018). https://doi.org/10.1080/01932691.2017.1398661
3. Hussin, M.H., Pohan, N.A., Garba, Z.N., Kassim, M.J., Rahim, A.A., Brosse, N., Yemloul, M., Fazita, M.R.N., Haafiz, M.K.M.: Physicochemical of microcrystalline cellulose from oil palm fronds as potential methylene blue adsorbents. Int. J. Biol. Macromol. **92**, 11–19 (2016). https://doi.org/10.1016/j.ijbiomac.2016.06.094

4. Biesheuvel, P.M., Porada, S., Elimelech, M., Dykstra, J.E.: Tutorial review of reverse osmosis and electrodialysis. J. Memb. Sci. **647**, 120221 (2022). https://doi.org/10.1016/j.memsci.2021.120221
5. Leiknes, T.O.: The effect of coupling coagulation and flocculation with membrane filtration in water treatment: A review. J. Environ. Sci. **21**, 8–12 (2009). https://doi.org/10.1016/S1001-0742(09)60003-6
6. Malaeb, L., Ayoub, G.M.: Reverse osmosis technology for water treatment: State of the art review. Desalination **267**, 1–8 (2011). https://doi.org/10.1016/j.desal.2010.09.001
7. Ganiyu, S.O., Sable, S., Gamal El-Din, M.: Advanced oxidation processes for the degradation of dissolved organics in produced water: A review of process performance, degradation kinetics and pathway. Chem. Eng. J. **429**, 132492 (2022). https://doi.org/10.1016/j.cej.2021.132492
8. Rayaroth, M.P., Aravindakumar, C.T., Shah, N.S., Boczkaj, G.: Advanced oxidation processes (AOPs) based wastewater treatment - unexpected nitration side reactions - a serious environmental issue: A review. Chem. Eng. J. **430**, 133002 (2022). https://doi.org/10.1016/j.cej.2021.133002
9. Costa, T.C., Hendges, L.T., Temochko, B., Mazur, L.P., Marinho, B.A., Weschenfelder, S.E., Florido, P.L., da Silva, A., Ulson de Souza, A.A., Ulson, Guelli, de Souza, S.M.A.: Evaluation of the technical and environmental feasibility of adsorption process to remove water soluble organics from produced water: A review. J. Pet. Sci. Eng. **208**, 109 (2022). https://doi.org/10.1016/j.petrol.2021.109360
10. Al-Muttair, A.K., Al Easawi, N.A.R., Mustafa, S.A.: Using Adsorption as Means to Treat Water Pollution. J. Biotechnol. Res. Cent. **16**, 37–47 (2022). https://doi.org/10.24126/jobrc.2022.16.1.627
11. Afroze, S., Sen, T.K.: A Review on Heavy Metal Ions and Dye Adsorption from Water by Agricultural Solid Waste Adsorbents. Water, Air, Soil Pollut. **229**, 225 (2018). https://doi.org/10.1007/s11270-018-3869-z
12. Boukoussa, B., Hamacha, R., Morsli, A., Bengueddach, A.: Adsorption of yellow dye on calcined or uncalcined Al-MCM-41 mesoporous materials. Arab. J. Chem. **10**, S2160–S2169 (2017). https://doi.org/10.1016/j.arabjc.2013.07.049
13. Lee, C.K., Liu, S.S., Juang, L.C., Wang, C.C., Lin, K.S., Lyu, MDu.: Application of MCM-41 for dyes removal from wastewater. J. Hazard. Mater. **147**, 997–1005 (2007). https://doi.org/10.1016/j.jhazmat.2007.01.130
14. Ewis, D., Ba-Abbad, M.M., Benamor, A., El-Naas, M.H.: Adsorption of organic water pollutants by clays and clay minerals composites: A comprehensive review. Appl. Clay Sci. **229**, 106686 (2022). https://doi.org/10.1016/j.clay.2022.106686
15. de Oliveira, E.H.C., Mendonça, É.T.R., Barauna, O.S., Ferreira, J.M., da Motta Sobrinho, M.A.: Study of variables for optimization of the dye indosol adsorption process using red mud and clay as adsorbents. Adsorption **22**, 59–69 (2016). https://doi.org/10.1007/s10450-015-9742-0
16. Sudan, S., Kaushal, J., Khajuria, A., Goyal, H., Mantri, A.: Bentonite clay-modified coconut biochar for effective removal of fluoride: kinetic, isotherm studies. Adsorption **30**, 389–401 (2024). https://doi.org/10.1007/s10450-024-00445-y
17. Zhu, R., Chen, Q., Zhou, Q., Xi, Y., Zhu, J., He, H.: Adsorbents based on montmorillonite for contaminant removal from water: A review. Appl. Clay Sci. **123**, 239–258 (2016). https://doi.org/10.1016/j.clay.2015.12.024
18. Peralta, M.E., Nisticò, R., Franzoso, F., Magnacca, G., Fernandez, L., Parolo, M.E., León, E.G., Carlos, L.: Highly efficient removal of heavy metals from waters by magnetic chitosan-based composite. Adsorption **25**, 1337–1347 (2019). https://doi.org/10.1007/s10450-019-00096-4
19. Wong, Y.C., Szeto, Y.S., Cheung, W.H., McKay, G.: Effect of temperature, particle size and percentage deacetylation on the adsorption of acid dyes on chitosan. Adsorption **14**, 11–20 (2008). https://doi.org/10.1007/s10450-007-9041-5
20. Salama, A.: Cellulose/silk fibroin assisted calcium phosphate growth: Novel biocomposite for dye adsorption. Int. J. Biol. Macromol. **165**, 1970–1977 (2020). https://doi.org/10.1016/j.ijbiomac.2020.10.074
21. Moradi, O., Panahandeh, S.: Fabrication of different adsorbents based on zirconium oxide, graphene oxide, and dextrin for removal of green malachite dye from aqueous solutions. Environ. Res. **214**, 114042 (2022). https://doi.org/10.1016/j.envres.2022.114042
22. Dominguez, M.A., Etcheverry, M., Zanini, G.P.: Evaluation of the adsorption kinetics of brilliant green dye onto a montmorillonite/alginate composite beads by the shrinking core model. Adsorption **25**, 1387–1396 (2019). https://doi.org/10.1007/s10450-019-00101-w
23. Edathil, A.A., Pal, P., Banat, F.: Alginate clay hybrid composite adsorbents for the reclamation of industrial lean methyldiethanolamine solutions. Appl. Clay Sci. **156**, 213–223 (2018). https://doi.org/10.1016/j.clay.2018.02.015
24. Gao, J., Yang, Q., Ran, F., Ma, G., Lei, Z.: Preparation and properties of novel eco-friendly superabsorbent composites based on raw wheat bran and clays. Appl. Clay Sci. **132–133**, 739–747 (2016). https://doi.org/10.1016/j.clay.2016.08.021
25. Hu, Y., Pan, C., Zheng, X., Liu, S., Hu, F., Xu, L., Xu, G., Peng, X.: Removal of Ciprofloxacin with Aluminum-Pillared Kaolin Sodium Alginate Beads (CA-Al-KABs): Kinetics, Isotherms, and BBD Model. Water **12**, 905 (2020). https://doi.org/10.3390/w12030905
26. Schmidt, L.N., Horst, M.F., Lencina, M.M.S., López, O.V., Ninago, M.D.: Gels based on calcium alginate/pillared bentonite: structural characterization and their use as cadmium removal agent. J. Environ. Sci. Heal. - Part A Toxic/Hazardous Subst. Environ. Eng. **57**, 218–228 (2022). https://doi.org/10.1080/10934529.2022.2050124
27. Sharifian, S., Asasian-Kolur, N., Najafi, H., Haddadi, B., Jordan, C., Harasek, M.: Reusable granulated silica pillared clay for wastewater treatment, selective for adsorption of Ni(II). Clean. Eng. Technol. **14**, 100634 (2023). https://doi.org/10.1016/j.clet.2023.100634
28. Han, Y.: Acidic and Hydrophobic Microporous Clays Pillared with Mixed Metal Oxide Nano-Sols. J. Solid State Chem. **144**, 45–52 (1999). https://doi.org/10.1006/jssc.1998.8115
29. Gimbert, F., Morin-Crini, N., Renault, F., Badot, P.M., Crini, G.: Adsorption isotherm models for dye removal by cationized starch-based material in a single component system: Error analysis. J. Hazard. Mater. **157**, 34–46 (2008). https://doi.org/10.1016/j.jhazmat.2007.12.072
30. Suwannahong, K., Wongcharee, S., Kreetachart, T., Sirilamduan, C., Rioyo, J., Wongphat, A.: Evaluation of the microsoft excel solver spreadsheet-based program for nonlinear expressions of adsorption isotherm models onto magnetic nanosorbent. Appl. Sci. **11**, 1–18 (2021). https://doi.org/10.3390/app11167432
31. Grishina, E.P., Ramenskaya, L.M., Kudryakova, N.O., Vagin, K.V., Kraev, A.S., Agafonov, A.V.: Composite nanomaterials based on 1-butyl-3-methylimidazolium dicianamide and clays. J. Mater. Res. Technol. **8**, 4387–4398 (2019). https://doi.org/10.1016/j.jmrt.2019.07.050
32. Zamouche, M., Hamdaoui, O.: Sorption of Rhodamine B by cedar cone: Effect of pH and ionic strength. In: Energy Procedia, pp. 1228–1239. Elsevier B.V (2012)
33. Giles, C.H., Smith, D., Huitson, A.: A general treatment and classification of the solute adsorption isotherm. I. Theoretical.

J. Colloid Interface Sci. **47**, 755–765 (1974). https://doi.org/10.1016/0021-9797(74)90252-5
34. Rangabhashiyam, S., Anu, N., Giri Nandagopal, M.S., Selvaraju, N.: Relevance of isotherm models in biosorption of pollutants by agricultural byproducts. J. Environ. Chem. Eng. **2**, 398–414 (2014). https://doi.org/10.1016/j.jece.2014.01.014
35. Tzabar, N., ter Brake, H.J.M.: Adsorption isotherms and Sips models of nitrogen, methane, ethane, and propane on commercial activated carbons and polyvinylidene chloride. Adsorption **22**, 901–914 (2016). https://doi.org/10.1007/s10450-016-9794-9
36. Raji, F., Saraeian, A., Pakizeh, M., Attarzadeh, F.: Removal of Pb(ii) from aqueous solution by mesoporous silica MCM-41 modified by ZnCl2: Kinetics, thermodynamics, and isotherms. RSC Adv. **5**, 37066–37077 (2015). https://doi.org/10.1039/c5ra01192b
37. Dávila-Jiménez, M.M., Elizalde-González, M.P., Peláez-Cid, A.A.: Adsorption interaction between natural adsorbents and textile dyes in aqueous solution. Colloids Surfaces A Physicochem. Eng. Asp. **254**, 107–114 (2005). https://doi.org/10.1016/j.colsurfa.2004.11.022
38. Jeffries, C.D.: Clays and Clay Minerals. Soil Sci. Soc. Am. J. **20**, 296–296 (1956). https://doi.org/10.2136/sssaj1956.03615995002000020037x
39. Bhattacharyya, K.G., SenGupta, S., Sarma, G.K.: Interactions of the dye, Rhodamine B with kaolinite and montmorillonite in water. Appl. Clay Sci. **99**, 7–17 (2014). https://doi.org/10.1016/j.clay.2014.07.012
40. Benjelloun, M., Miyah, Y., Akdemir Evrendilek, G., Zerrouq, F., Lairini, S.: Recent Advances in Adsorption Kinetic Models: Their Application to Dye Types. Arab. J. Chem. **14**, 103031 (2021). https://doi.org/10.1016/j.arabjc.2021.103031
41. Yousef, R.I., El-Eswed, B., Al-Muhtaseb, A.H.: Adsorption characteristics of natural zeolites as solid adsorbents for phenol removal from aqueous solutions: Kinetics, mechanism, and thermodynamics studies. Chem. Eng. J. **171**, 1143–1149 (2011). https://doi.org/10.1016/j.cej.2011.05.012
42. Qin, Q., Ma, J., Liu, K.: Adsorption of anionic dyes on ammonium-functionalized MCM-41. J. Hazard. Mater. **162**, 133–139 (2009). https://doi.org/10.1016/j.jhazmat.2008.05.016
43. Ghosal, P.S., Gupta, A.K.: An insight into thermodynamics of adsorptive removal of fluoride by calcined Ca-Al-(NO3) layered double hydroxide. RSC Adv. **5**, 105889–105900 (2015). https://doi.org/10.1039/c5ra20538g
44. Tunioli, F., Khaliha, S., Mantovani, S., Bianchi, A., Kovtun, A., Xia, Z., Bafqi, M.S.S., Okan, B.S., Marforio, T.D., Calvaresi, M., Palermo, V., Navacchia, M.L., Melucci, M.: Adsorption of emerging contaminants by graphene related materials and their alginate composite hydrogels. J. Environ. Chem. Eng. **11**, 109566 (2023). https://doi.org/10.1016/j.jece.2023.109566
45. Kaushal, M., Tiwari, A.: Removal of rhodamine-b from aqueous solution by adsorption onto crosslinked alginate beads. J. Dispers. Sci. Technol. **31**, 438–441 (2010). https://doi.org/10.1080/01932690903210135
46. Xiao, D., He, M., Liu, Y., Xiong, L., Zhang, Q., Wei, L., Li, L., Yu, X.: Strong alginate/reduced graphene oxide composite hydrogels with enhanced dye adsorption performance. Polym. Bull. **77**, 6609–6623 (2020). https://doi.org/10.1007/s00289-020-03105-7
47. Lui, F., Zhang, H., Zhu, L., Liao, Y., Nawaz, F., Meng, X., Xiao, F.-S.: High-temperature hydrothermal synthesis of magnetically active ordered mesoporous resin and carbon monoliths with reusable adsorption for organic dye. Adsorption **19**(1), 39–47 (2013). https://doi.org/10.1007/s10450-012-9408-0
48. Jedynak, K., Wideł, D., Rędzia, N.: Removal of rhodamine B (A basic dye) and acid yellow 17 (An acidic dye) from aqueous solutions by ordered mesoporous carbon and commercial activated carbon. Colloids Interfaces **3**(1), 30 (2019). https://doi.org/10.3390/colloids3010030
49. Selvam, P.P., Preethi, S., Basakaralingam, P., Thinakaran, N., Sivasamy, A., Sivanesan, S.: Removal of rhodamine B from aqueous solution by adsorption onto sodium montmorillonite. J. Hazard. Mater. **155**, 39–44 (2008). https://doi.org/10.1016/j.jhazmat.2007.11.025
50. Zimmermann, B.M., Dotto, G.L., Kuhn, R.C., Mazutti, M.A., Treichel, H., Foletto, E.L.: Adsorption of hazardous dye Rhodamine B onto Brazilian natural bentonite. Int. J. Environ. Technol. Manag. **19**, 1–15 (2015). https://doi.org/10.1504/IJETM.2016.074798
51. Etcheverry, M., Cappa, V., Trelles, J., Zanini, G.: Montmorillonite-alginate beads: Natural mineral and biopolymers based sorbent of paraquat herbicides. J. Environ. Chem. Eng. **5**, 5868–5875 (2017). https://doi.org/10.1016/j.jece.2017.11.018
52. Sabarish, R., Unnikrishnan, G.: Novel biopolymer templated hierarchical silicalite-1 as an adsorbent for the removal of rhodamine B. J. Mol. Liq. **272**, 919–929 (2018). https://doi.org/10.1016/j.molliq.2018.10.093
53. Chang, N.B., Houmann, C., Lin, K.S., Wanielista, M.: Fate and transport with material response characterization of green sorption media for copper removal via desorption process. Chemosphere **154**, 444–453 (2016). https://doi.org/10.1016/j.chemosphere.2016.03.130
54. Azizian, S., Bashiri, H.: Description of desorption kinetics at the solid/solution interface based on the statistical rate theory. Langmuir **24**, 13013–13018 (2008). https://doi.org/10.1021/la8029769
55. Larasati, A., Fowler, G.D., Graham, N.J.D.: Insights into chemical regeneration of activated carbon for water treatment. J. Environ. Chem. Eng. **9**, 105555 (2021). https://doi.org/10.1016/j.jece.2021.105555